






Article

Valorization of Face Masks Produced during COVID-19 Pandemic through Hydrothermal Carbonization (HTC): A Preliminary Study

Gianluigi Farru ^{1,*}, Judy A. Libra ², Kyoung S. Ro ³, Carla Cannas ⁴, Claudio Cara ⁴, Aldo Muntoni ^{1,5}, Martina Piredda ¹ and Giovanna Cappai ^{1,5,*}

¹ Department of Civil-Environmental Engineering, University of Cagliari, Via Marengo 2, 09123 Cagliari, Italy

² Leibniz Institute of Agricultural Engineering and Bio-Economy e.V. (ATB), Max-Eyth-Allee 100, 14469 Potsdam, Germany

³ Coastal Plains Soil, Water & Plant Research Center, United States Department of Agriculture (USDA) Agricultural Research Service (ARS), 2611 W. Lucas St., Florence, SC 29501, USA

⁴ Department of Chemical and Geological Sciences, University of Cagliari, University Campus, Monserrato, 09042 Cagliari, Italy

⁵ IGAG-CNR—Institute of Environmental Geology and Geoengineering, National Research Council, Via Marengo 2, 09123 Cagliari, Italy

* Correspondence: gianluigi.farru@unica.it (G.F.); gcappai@unica.it (G.C.)

Abstract: The COVID-19 pandemic has led to the increased use of disposable face masks worldwide, resulting in a surge of potentially infectious waste. This waste must be safely managed and disposed of to prevent the spread of the virus. To address this issue, a preliminary study explored the use of hydrothermal carbonization (HTC) as a potential method for converting surgical mask waste into value-added carbonaceous materials. The HTC treatments were conducted at 220 °C for 3 h with or without the addition of acetic acid. The resulting hydrochar was characterized using several techniques, including thermogravimetric analysis (TGA), scanning electron microscopy (SEM), Fourier transform infrared spectroscopy (FTIR), and N₂-physisorption analyzers. The study found that the masks formed a melt with reduced mass (−15%) and volume (up to −75%) under the applied conditions. The carbon content and higher heating value (HHV) of the produced hydrochars were higher than those of the original masks (+5%). Furthermore, when acetic acid was added during the HTC experiment, a new crystal phase, terephthalic acid, was produced. This acid is a precursor in surgical mask production. The study suggests that hydrothermal carbonization could potentially achieve sanitization and volume reduction in non-renewable and non-biodegradable surgical masks while also producing a solid fuel or a raw material for terephthalic acid production. This approach offers an innovative and sustainable solution to manage the waste generated by the increased use of disposable face masks during the pandemic.

Keywords: hydrothermal carbonization; surgical mask; waste management; waste valorization; solid fuel; value-added chemicals



Citation: Farru, G.; Libra, J.A.; Ro, K.S.; Cannas, C.; Cara, C.; Muntoni, A.; Piredda, M.; Cappai, G.

Valorization of Face Masks Produced during COVID-19 Pandemic through Hydrothermal Carbonization (HTC): A Preliminary Study. *Sustainability* **2023**, *15*, 9382. <https://doi.org/10.3390/su15129382>

Academic Editor: Maurizio Volpe

Received: 2 May 2023

Revised: 3 June 2023

Accepted: 7 June 2023

Published: 10 June 2023



Copyright: © 2023 by the authors. Licensee MDPI, Basel, Switzerland. This article is an open access article distributed under the terms and conditions of the Creative Commons Attribution (CC BY) license (<https://creativecommons.org/licenses/by/4.0/>).

1. Introduction

The COVID-19 pandemic has significantly impacted various aspects of daily life worldwide. The rapid growth in infection in many countries has led to the introduction of numerous rules and restrictions aimed at protecting human health and life. Since the transmission and spreading of the COVID-19 virus are mainly due to the droplets of saliva released by an infected person through coughs or sneezes [1], it became essential to prevent the infections through the use of personal protective equipment (PPE), such as masks, surgical gloves, face shields, goggles, and gowns [2,3]. Especially, face masks have become the first prevention measure used to fight the virus spreading worldwide and are, nowadays, everyday items, as well as phones, clothes, accessories, etc. [4]. Based

on the filtration capacity and the sealing ability towards stopping respiratory droplets, different types of masks are available in the market. The Filtered Face Piece FFP2 type is a high-efficiency mask in terms of protection, wearability, and ease of breathing, specifically aimed at protecting the wearer. It is generally made of five layers of polypropylene (PP) and polyethylene (PE), an ear strap made of polyamide and a nose wire (generally steel made). However, due to the lower economic cost, the most widespread masks are the surgical type (3-ply type) characterized by good filtration capacity, hypoallergenic feature, cheaper price, and lower breathing resistance, mainly aimed at protecting other people from a potential transmission by the mask wearer [5,6]. They consist of three non-woven fabric layers mainly composed of polypropylene. Other plastic materials such as polystyrene, polycarbonate, polyethylene, or polyester are also applied to increase mask density.

Wearing face masks has been demonstrated to be very effective and easy to cut down transmission routes, but their single-use nature results in the generation of massive amount of potentially infectious plastic waste. In the event of a prolonged pandemic situation, estimation on the average use of disposable face masks by the global population indicates the need of 1097 billion masks per year, which corresponds to 8388 thousand tons of produced waste masks requiring proper management [7]. The disposal methods applied so far to potentially infectious waste are incineration, mainly aimed at killing pathogens and sanitary landfill after steaming and boiling at a high temperature [2,8]. However, these methods are not sustainable nor contribute to the circular economy principles, aimed at reducing/preventing negative environmental impacts with the recovery of high-value resources. Conversely, the progressive depletion of global resources in a context of increasing demand requires identifying new approaches for waste valorization as a potential resource. This is particularly pertinent in the current COVID-19 pandemic situation where health and safety concerns pose new challenges in terms of both resources supply and waste management. Therefore, a robust and flexible recycling method which can deal with very large amounts of waste characterized by an infectious risk and by the presence of several types of plastic polymer is urgently needed.

Plastics, specifically polypropylene, which represents 30% of the overall plastic production, are at present widely used and have become a primary support for the modern lifestyle due to their low cost of production and a wide range of relevant properties such as low density, durability, and corrosion resistance. However, the widespread use of plastic items poses a major environmental challenge due to the resulting huge amounts of waste characterized by low biodegradability. Mixed-plastic items may contain various polymers such as polyethylene (PE), polypropylene (PP), polyethylene terephthalate (PET), polyvinyl chloride (PVC), polystyrene (PS), polycarbonate (PC), and more. Although the various polymers exhibit so different chemical–physical properties that recycling is difficult in the absence of a preliminary separation, common characteristic features shared among all of them are high volatile matter contents, high viscosity at low melting points, and high energy density due to high carbon contents along with very low moisture and ash contents. Several studies have been investigating the application of thermochemical technologies such as liquefaction, gasification, or co-pyrolysis at higher temperatures to convert mixed-plastic wastes into fuels (e.g., gas and oil) with higher calorific values or carbon-enriched material [9–12]. In this respect, recently, potential production of value-added carbonaceous material by hydrothermally carbonizing plastic waste is gaining interest [13]. Hydrothermal carbonization (HTC) is a thermochemical conversion process that can be used to obtain energy or new materials from organic matrices in the presence of pressurized water under subcritical conditions. This technology aims to produce a carbon-rich product, called hydrochar, which can be used as a solid fuel, environmental adsorbent, and soil amendment. Moreover, the HTC process proved to remove pathogens and antibiotic resistance genes (ARGs), for example, from animal carcasses [14]. To date, HTC has been extensively applied to residual biomass characterized by high water content as, contrary to treatments such as pyrolysis or gasification, the presence of water is functional to the process and, therefore, preliminary drying is not required [15,16]. In contrast, only a few

studies have been carried out on synthetic polymers [13,17]. It is our opinion that, the ability to treat carbonaceous matrices of various kinds and to eliminate pathogens [14], as well as the potential adoption in decentralized utilities, makes HTC suitable for the treatment and valorization of disposable masks containing different plastic polymers.

Based on these premises, this work evaluates the preliminary feasibility of converting single-use masks into value-added products through hydrothermal carbonization. To the best of the authors' knowledge, hydrothermal carbonization has never been used to treat this kind of waste. The HTC process has been carried out on used masks in the presence and the absence of acetic acid at 220 °C for 3 h. The addition of acid in HTC treatment is frequently presented in the literature to improve/accelerate the HTC reactions. Poerschmann et al. (2015) treated PVC (polyvinyl chloride) with the presence of citric acid reporting and reported that no significant change was observed in the products. However, when lignocellulosic biomass and plastic material were hydrothermally carbonized together (i.e., co-HTC), organic acids (e.g., acetic acid) were produced by the lignocellulosic material degradation, increasing the overall performance in the treatment of the plastic material by removing inorganic salts from the hydrochar, which would complicate its combustion [17–20]. The temperature and holding time were selected by considering the findings from various studies in the literature that investigated different conditions. Based on their results, the optimal conditions identified for treating our plastic residues were selected to be 220 °C for a holding time of 3 h [18,21,22]. To the best of our knowledge, the HTC process has so far never been applied to PPE; consequently, this work aims to provide a first and preliminary contribution to exploring the potential role of HTC in the suitable management of waste masks.

2. Materials and Methods

Used 3-ply masks (Figure 1), consisting of filtering layers made of PP (88.5%wt) and ear straps made of polyester (11.5%wt), were collected and sterilized in a bath of sodium hypochlorite (0.5% *v/v*) for safe handling. After a few days, the sterilized masks were washed with distilled water and dried in the air. Subsequently, the metal parts of the masks that were designed to conform to the shape of the nose were removed. The HTC experiments were carried out with a L/S (liquid-to-solid) ratio of 10 L/kg, at a temperature of 220 °C and a holding time of 3 h. Pure distilled water (pH of 6.11) and distilled water containing 5% *v/v* of glacial acetic acid (pH of 2.58) were used as the liquid medium. All tests were performed in triplicate.



Figure 1. Used mask collected for HTC experiments.

The HTC process was carried out in a 1 L stainless-steel pressurized and thermostated reactor (Berghof GmbH, Eningen, Germany). The solid material was completely immersed in the medium, and the reactor was sealed using a polytetrafluoroethylene (PTFE) gasket. The system was heated from ambient temperature to 220 °C and held at this temperature for the set treatment time of 3 h. At the end of the treatment, the electric heater was turned off, and the whole device was cooled gradually down to ambient temperature. Once the reactor had cooled, most of the solid phase product (hydrochar) was manually separated from the process water (PW) using a lab tong; the remaining share was recovered by filtration using a cellulose nitrate filter with a pore size of 0.45 µm. The solid product was thoroughly dried in a ventilated oven at 105 °C then stored in plastic bags, while the liquid phase was collected in plastic bottles and stored at 4 °C until characterization.

Process water and solid products deriving from HTC experiments in the presence or absence of acetic acid (identified in the following by the abbreviation MA and M, respectively) were chemically and physically characterized, including macro-elements (C, H, N), ash content, higher heating value (HHV), and lower heating value (LHV). The latter was calculated by subtracting the heat energy required to vaporize the water formed during the combustion process. In addition, Fourier-transform infrared spectroscopy (FTIR), scanning electron microscopy (SEM), and N₂-physisorption measurements were applied to the solid fraction. The process water was analyzed for pH, electrical conductivity (EC), density, total carbon (TC), inorganic carbon (IC), and total organic carbon (TOC). Ultimate analysis for carbon, hydrogen, and nitrogen content was performed using a CHN analyzer (LECO 628); oxygen concentration was determined by difference. Electrical conductivity and pH were measured using a benchtop meter (model HI 5521-01, Hanna Instruments S.R.L., Nusfalau, Romania). Total organic carbon (TOC), as well as inorganic carbon (IC) contents, were assessed using a total organic carbon analyzer (TOC-VCSN, Shimadzu Corporation, Kyoto, Japan).

As for the solid materials, thermal analysis was carried out by a thermogravimetric analyzer (TGA), where oxygen (40 mL/min) was used, and a heating ramp from 25 °C to 900 °C (rate of 10 °C/min) was applied (PerkinElmer STA 6000, Waltham, MA, USA), estimating volatile matter, ash content, and fixed carbon according to the TGA results. The higher heating value was estimated with an adiabatic calorimeter (LECO AC500, St. Joseph, MI, USA). The H/C (hydrogen/carbon) and O/C (oxygen/carbon) atomic ratios were assessed for both the original material and the obtained hydrochar. X-ray diffraction (XRD) analysis was carried out with a PXRD Diffractometer (Panalytical Xpert Pro) equipped with Cu anode, and the Fourier-transform infrared spectroscopy (FTIR) with a Jasco FT-IR6300A spectrometer equipped with an ATR PRO ONE (diamond crystal) in the 4000–400 cm⁻¹ spectral range (res. 4.0 cm⁻¹, 50 scans). Finally, SEM analysis was carried out using a scanning electron microscope Quanta 200 ESEM (FEI Company, Hillsboro, OR, USA) working in low vacuum conditions.

N₂-physisorption analyses were carried out with Quantachrome NOVAtouch LX4, The Brunauer–Emmett–Teller (BET) specific surface area was calculated from the adsorption data in the p/p₀ range 0.05–0.3 and microporous and mesoporous volume was calculated at p/p₀ = 0.9.

The hydrochar mass yield was evaluated by carefully weighing the dried samples and subsequently performing mass and energy balances, according to Equation (1).

$$\text{Mass Yield} = (\text{Mass of hydrochar}) / (\text{Mass of raw sample}) \cdot 100\% \quad (1)$$

The energy yield was calculated based on the mass yield and the higher heating values (HHVs) assessed for the hydrochar and the raw sample, according to Equation (2).

$$\text{Energy Yield} = \text{Mass Yield} \cdot (\text{HHV of hydrochar}) / (\text{HHV of raw sample}) \cdot 100\% \quad (2)$$

Results were validated through ANOVA (analysis of variance) using JMP statistical software (SAS, v.16).

3. Results and Discussion

The hydrochars obtained from the HTC treatment of masks with and without acetic acid (labelled with MA and M, respectively) are illustrated in Figure 2a,b. Under the applied conditions, a melt was formed, having a very different physical appearance from the source material. Interestingly, the hydrochars produced during the test with acetic acid (Figure 2b) possessed very different macroscopic characteristics from those produced without acid (Figure 2a), indicating that acetic acid influences the HTC reactions and consequently might lead to different transformations of the original materials. The M hydrochars were compact porous solids, whilst in MA hydrochars (Figure 2b), two different solid phases can be recognized: a porous solid and a crystal phase (as detailed in Figure 2c). The M hydrochar retained the blue color of the original mask while the MA hydrochar lost most of its color, indicating the loss of chromophores due to the presence of acids.

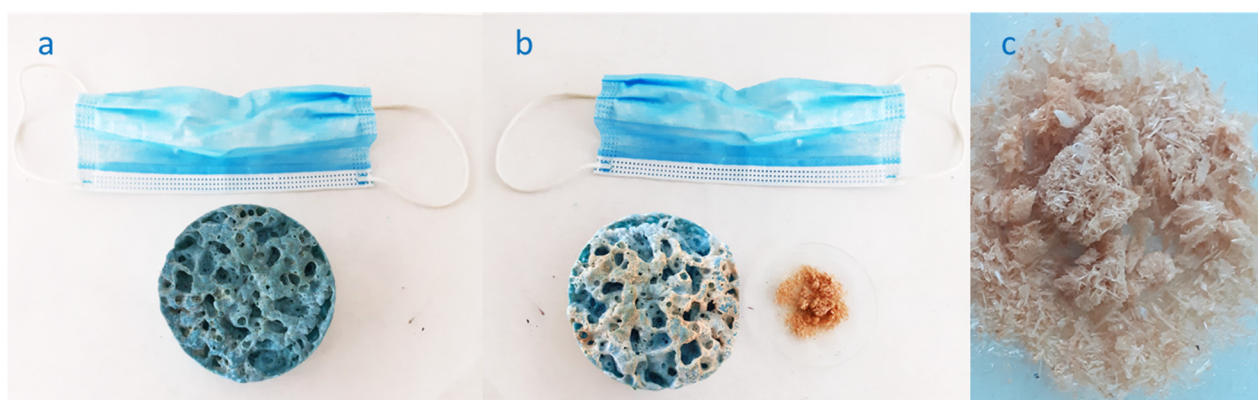


Figure 2. Surgical mask and produced hydrochars: (a) M, (b) MA, and (c) detail of MA crystals.

The solid mass yields were 89.06 and 83.61% for M and MA, respectively, higher than that for hydrochars derived from biogenic materials [16].

Results of the feedstock masks and the hydrochar characterization are shown in Table 1 and Figure 3. In the HTC treatment increased carbon and hydrogen contents while oxygen content decreased. The highest increase in carbon and hydrogen contents was attained for MA (8.14 and 10.73%, respectively). In addition to oxygen, HTC also reduced the ash content to very small percentages compared to that of the original masks (Table 1). The highest decrease was assessed for M (−89.06%), and it may be attributed to the dissolution of inorganic compounds into the water.

Table 1. Elemental composition, ash content (% dry basis), atomic ratios H/C and O/C, HHV, LHV, and Energy yield of the samples.

Sample	Ash [%]	C [%]	H [%]	N [%]	O [%]	H/C [-]	O/C [-]	HHV [MJ/kg]	LHV [MJ/kg]	Energy Yield [-]
Masks	1.92 (0.04)	76.21 (0.89)	12.02 (0.53)	2.08 (0.20)	7.77 (1.22)	1.892	0.077	43.12 (0.51)	40.48	-
M	0.21 (0.02)	82.99 (1.14)	13.22 (0.35)	0.17 (0.03)	3.41 (1.47)	1.911	0.031	45.29 (0.21)	42.41	0.94
MA	0.59 (0.04)	82.41 (0.09)	13.31 (0.19)	0.17 (0.04)	3.68 (0.26)	1.938	0.032	45.33 (0.17)	42.41	0.88

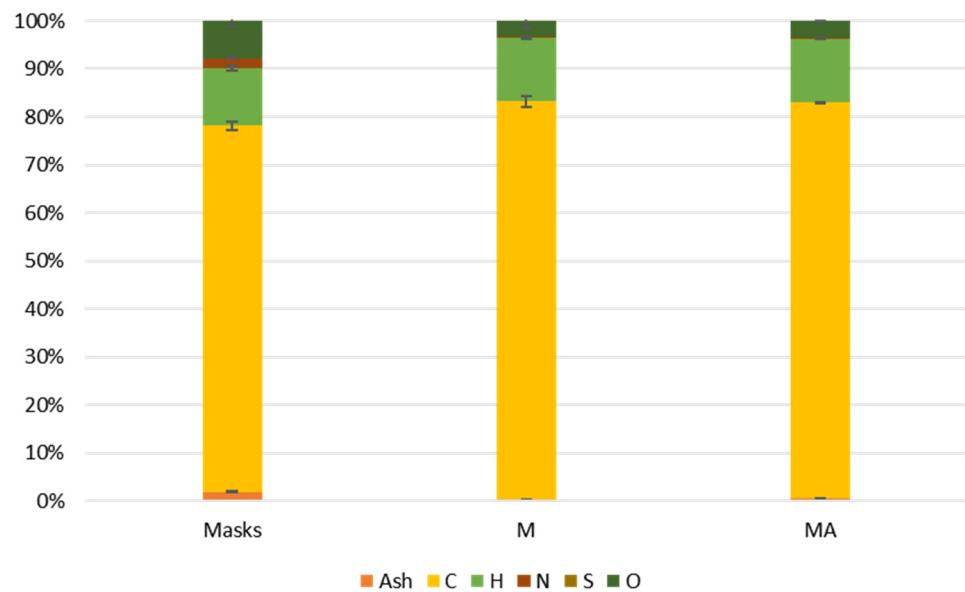


Figure 3. HTC solid products and raw material composition—percentage values.

The higher percentage of carbon and a lower percentage of oxygen in hydrochar can result from dehydration and decarboxylation processes typically occurring during HTC treatments. Generally, these reactions remove hydrogen and oxygen from the solid matrix in the form of H_2O and CO_2 [16]. The above-mentioned transformations can be visually described by the Van Krevelen diagram, in which the molar ratios H/C and O/C for the feedstock and the HTC products are represented (Figure 4). In this diagram, the intensity of the carbonization process is shown by the distance at which the carbonization products are located with respect to the source materials. Typically, during HTC experiments carried out on biomass, as the carbonization intensity increases, the H/C and O/C molar ratios of the hydrochars move from upper right to lower left [23]. In the case of masks, both the original materials and HTC products have much lower O/C ratios than common biomass and are located in the diagram in the typical fuel zone (such as gasoline, diesel, kerosene, biodiesel, and crude oil [24,25]). The HTC process only reduces the atomic ratio O/C , while the H/C values remain constant, indicating reduction reactions dominated over dehydrogenation reactions.

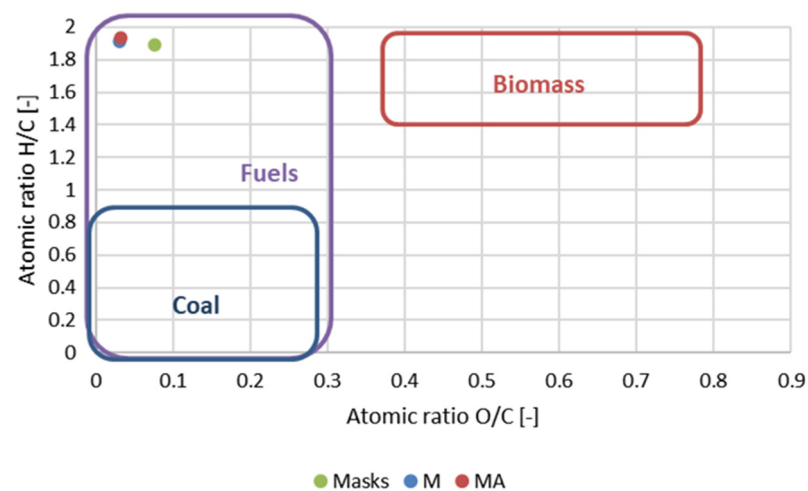


Figure 4. Van Krevelen diagram for masks and HTC products. In the graph, typical areas for biomass, fuels, and coal are marked. The fuels' area groups both liquid (kerosene, oil, diesel, etc.) and solid (coal, plastic materials, etc.) common fuels [24,25].

The HHV (Table 1) assessed for masks is similar to that of PP (45.77–46.24 MJ/kg) [26], comparable to that of common fuels such as diesel (44.80 MJ/kg), and even higher than anthracite (32.50 MJ/kg) [27]. After HTC treatment, HHV increased by approximately 5% (5.03 and 5.13% for M and MA, respectively). These results are significantly different from the values for the masks ($p < 0.01$), while M and MA are not statistically different. This is an interesting result in view of hydrochar valorization for energy recovery purposes. The energy yields obtainable with the combustion of the produced hydrochars are slightly lower than 1, due to the partial reduction in the mass during the HTC process and only slight increase in HHV. However, the energy density for the obtained hydrochars is enhanced due to the remarkable volume reduction caused by the HTC treatment, roughly estimated to be over 75% (Figure 5). When assessing the feasibility of HTC process, this positive aspect should be taken into consideration along with the disinfection of the spent masks, because the higher the energy density of the fuel, the more energy may be stored or transported by the same volume.



Figure 5. Volume reduction achieved for 20 masks through HTC.

Analysis such as TGA, PXRD (powder X-ray diffraction), FTIR, SEM, and N_2 -physisorption carried out on the source materials and the produced hydrochars highlighted the transformations that occurred during the HTC process. As shown in Figure 6, the results from TGA carried out on masks and on the solid products obtained during HTC indicate that the chemical composition of the masks was altered based on the different thermal decomposition patterns and ash contents. For instance, by comparing the thermal decomposition curves of mask and that of M and MA hydrochars, different decomposition temperatures are seen, which indicates that original polymers were altered and converted into new carbon materials. The masks decomposed in two regions with peak temperatures of 305 and 475 °C and with a residual mass of 1.92%. Different peak temperatures may be found in the literature depending on the additives used by the masks manufacturers. Consistent with our results, Ali et al. (2022) found a main single degradation stage in the range of 330 and 480 °C for PP layers of surgical masks with a heating rate of 10 °C/min [28]. However, in the study of Brillard et al. (2021), the peak temperatures of 3-layer surgical mask made of entirely polypropylene were higher than in our study (448 to 472 °C), whilst similar values were obtained for 3-layered masks made of cotton, polyethylene terephthalate, and polyamide: (354 to 382 °C for the 1st decomposition region and 424 to 459 °C for the 2nd decomposition region depending on heating rates from 5 to 20 °C/min) [9]. Yousef et al. (2021) reported similar peak temperatures (448 to 476 °C) for the 3-layer surgical mask decomposition using heating rates from 5 to 30 °C/min [4]. The major peak decomposition temperatures of hydrochar increased to 352 °C, 339 °C, and 356 °C for M, MA, and MA crystals, respectively. It is interesting to note that the residual mass decreased from 1.92% for raw mask to less than 0.59% for the derived hydrochar, suggesting the dissolution of inorganic ash chemicals into water during HTC treatment.

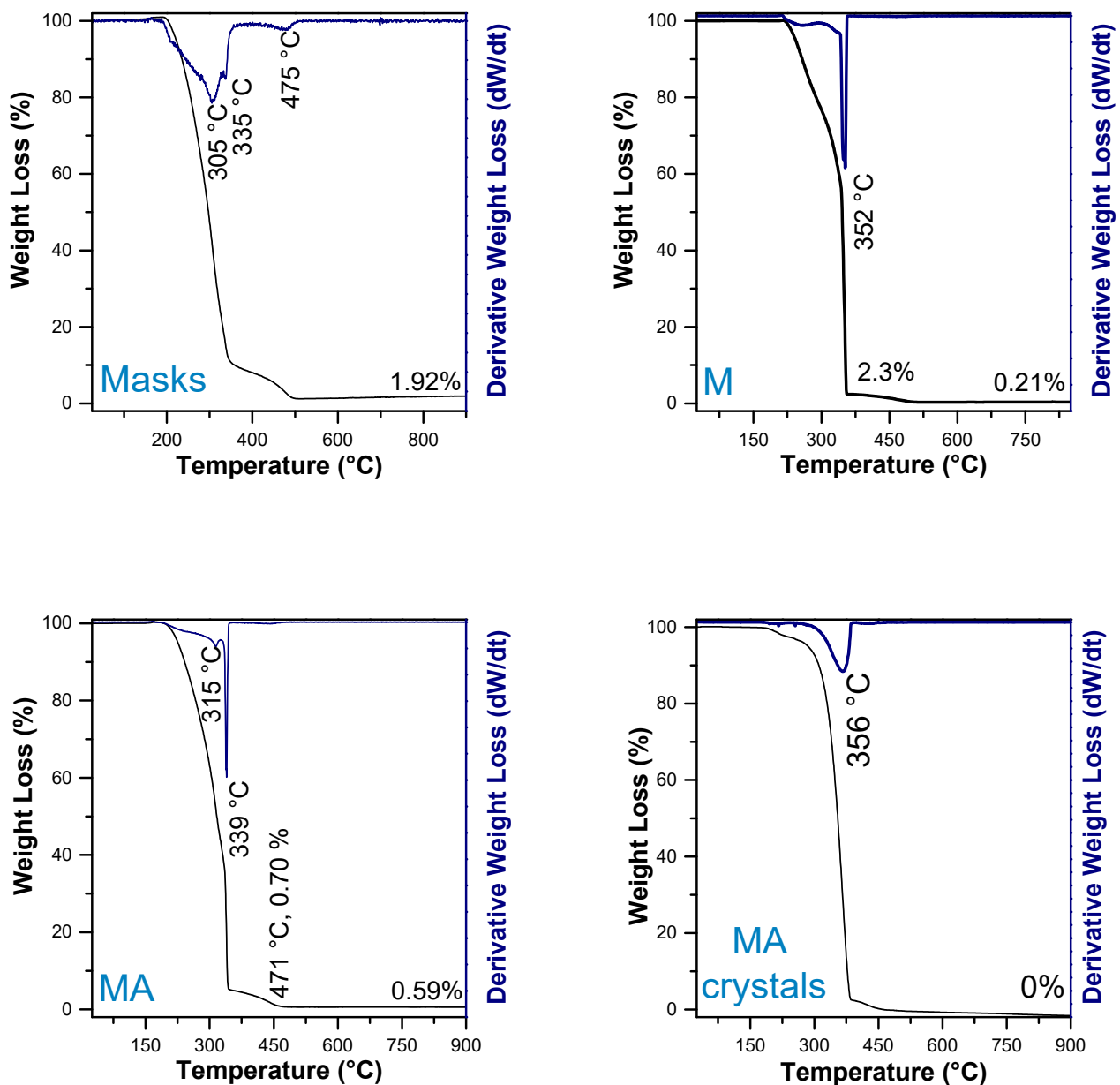


Figure 6. Thermogravimetric curves of surgical masks and their HTC products.

Figure 7 illustrates the results of FTIR analyses on masks and their HTC products. The area between 1800 and 2400 cm^{-1} is not considered because it is influenced by background noise. More specifically, Figure 7a shows a comparison between masks and polypropylene (PP), indicating a close similarity between the two spectra. In Figure 7b, a comparison is made between masks and the M and MA hydrochars. As a result of HTC, the spectrum of the source material is partially modified since new peaks are formed, and some others disappear. In detail, the broad bend at around 3400 cm^{-1} , generally associated with OH stretching, is reduced in the spectra of HCs and in PP. The peaks related to CH group vibrations are present in all spectra as sharp peaks (around 2951 – 2853 cm^{-1} , 1457 and 1375 cm^{-1} , and 999 , 971 , and 841 cm^{-1}) [29], while the peak associable to C=O at 1736 cm^{-1} is evident in the mask and PP spectra while in HC spectra disappears and a new peak on the right (1682 cm^{-1}), possibly related to C=C, appears. Finally, the peak at 1165 cm^{-1} may be related to C-O [30]. In Figure 7c, the spectra of the ear strap (polyester fabric) and PET are compared, showing a close match. The band at 2965 cm^{-1} can be related to the CH_2 stretching. The major peak at 1712 cm^{-1} can be attributed to the stretching of carboxylic

group C=O), while the peaks at 1339, 1240, and 1092 cm^{-1} are due to the C-O-C bonds. The sharp peak at 719 cm^{-1} may be caused by the C-H vibration in the aromatic ring. A similar spectrum for ear straps was reported by Ali et al. (2022) [28].

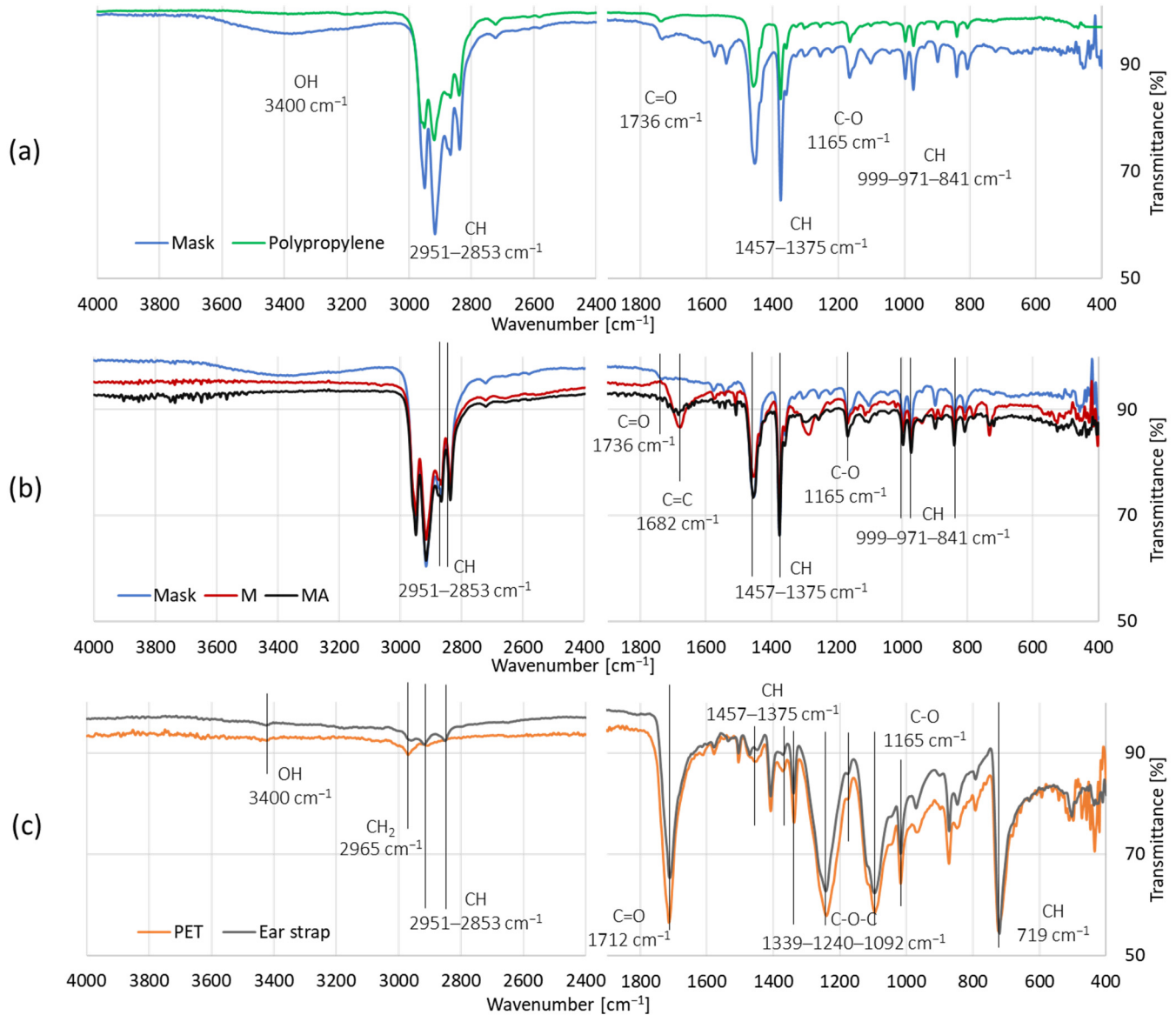


Figure 7. FTIR spectra of (a) surgical mask and polypropylene, (b) surgical mask and HTC solid products, and (c) ear strap and PET.

Powder X-ray Diffraction analysis was particularly useful in detecting the nature of crystals formed during MA test. In Figure 8, a comparison of the XRD patterns of M, MA, and crystals produced during MA test is reported. M and MA patterns are almost overlapping, indicating the presence of a unique phase of polypropylene [31]. The pattern of crystals obtained for MA corresponds to terephthalic acid (TPA) (PDF-Card 00-021-1919). This is in agreement with the TGA analysis of MA crystals that show a decomposition temperature compatible with terephthalic acid [32], a precursor of polyethylene terephthalate and other polyesters in the manufacturing process of the synthetic fibers [33,34]. Based on these results, it can be deduced that the presence of acetic acid allowed a more radical transformation of the material and TPA production is likely due to the decomposition in presence of acetic acid of ear straps (PET made). This is consistent with the results found in the literature reporting TPA production through PET depolymerisation [35–37].

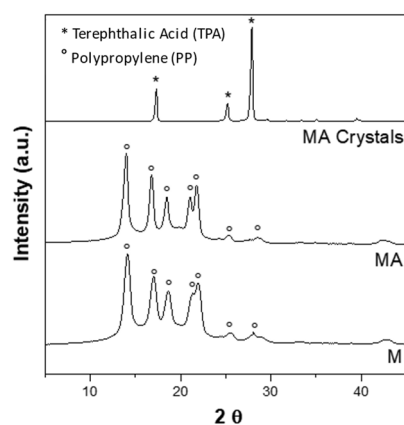


Figure 8. XRD patterns of M and MA hydrochar and crystals produced during MA HTC test. Peaks related to TPA (marked with *) and PP (marked with °) can be recognized in the patterns obtained for MA crystals and MA and M, respectively.

In order to assess whether the hydrothermal treatment on the surgical mask caused a modification of the textural properties, in terms of specific surface area, porous distribution and porous volume, N_2 -physorption analyses were carried out on the raw surgical masks and on the two hydrochars, M and MA. The obtained adsorption–desorption isotherms (Figure 9) of the surgical mask and the two hydrochars are ascribable to non-porous material in the micro-meso range, given the absence of capillary condensation in the entire isotherm. The specific surface area and microporous and mesoporous volume of the produced M and MA were 37.7 and 24.5 m^2/g with a micro-mesoporous volume of 0.03 and 0.02 cm^3/g , respectively (Table 2). The values remained in the range of the raw masks with a surface area of 44 m^2/g and a porous volume of 0.03 cm^3/g . The slight decrease in surface area and porous volume of M or MA hydrochars is probably attributable to the deformation of woven fiber of the face mask (Figure 10). Scanning Electron Microscopy analysis, however, showed evidence of a significant transformation in the physical structure of the masks following the HTC treatment. The fibers of non-woven fabric recognizable in masks (Figure 10a) were destroyed during the process, both in the absence and presence of acetic acid (Figure 10b,c). Figure 10d shows crystals of terephthalic acid formed in the presence of acetic acid. Overall, the chemical and physical structure of surgical masks was significantly altered by HTC.

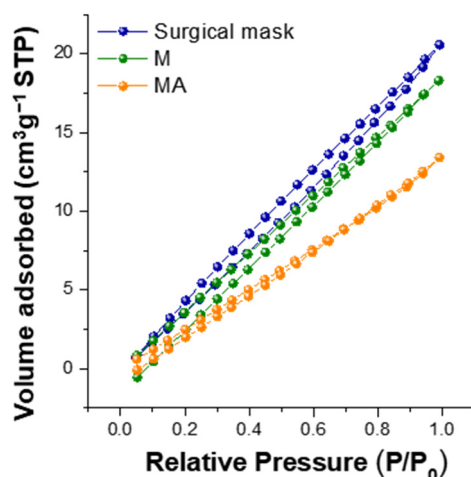


Figure 9. Adsorption–desorption isotherms of the samples M, MA, and the raw surgical mask.

Table 2. Specific surface area and micro-mesoporous volume values of the samples M, MA, and the raw surgical mask.

Sample	Surface Area [m ² /g]	Micro-Mesoporous Volume [cm ³ /g]
Surgical mask	44.0	0.03
M	37.7	0.03
MA	24.5	0.02

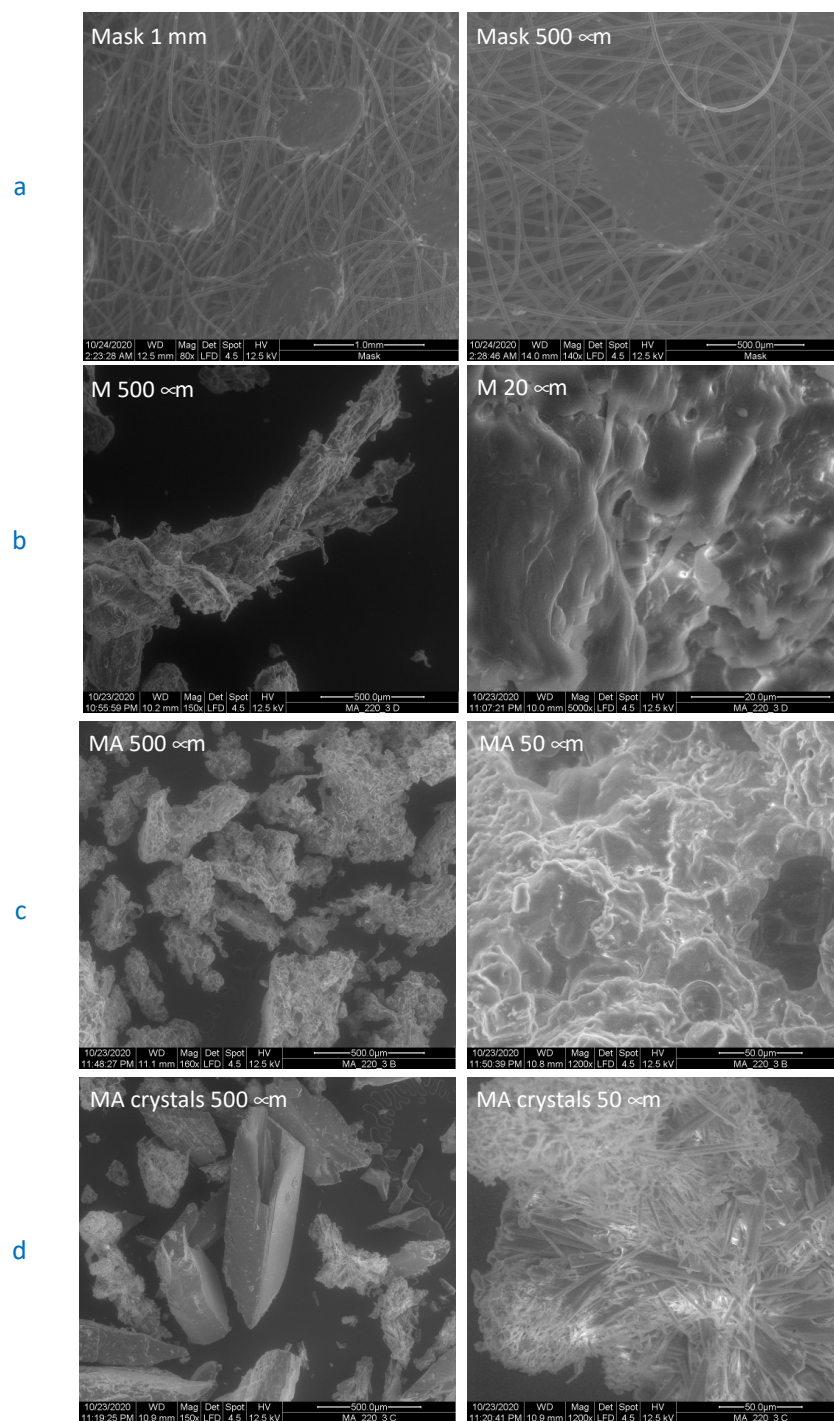
**Figure 10.** SEM imaging of (a) surgical mask and HTC solid product: (b) M hydrochar, (c) MA hydrochar, and (d) MA crystals.

Table 3 shows the results of analyses performed on the liquid phase obtained before and after the HTC treatments. The pH decreased from 6.11 to 3.82 in the HTC test carried out in the absence of acetic acid, while for the test with acetic acid, the pH remained low (from 2.52 to 2.7). The increase in EC indicates the dissolution of inorganics, which is consistent with the reduction in ash content in the solid product, a feature that is also underlined by the TGA results. The total organic carbon values were strongly influenced by the addition of acetic acid. While the HTC test with acetic acid started at a high initial TOC value in the liquid phase of ca. 20 g/L, the high amount of TOC in the process liquid after HTC indicates that more organic compounds are degraded from the solid matrices in the presence of acetic acid than without. By performing the C balance, the sum of the total carbon found in the solid and in the liquid phases was close to the total input carbon from the masks; therefore, there was no evidence of gas formation, as confirmed by the final pressure in the reactor, which was $P = 1$ atm.

Table 3. Liquid phase characterization—pH, electrical conductivity, and carbon content in the process water before and after the HTC treatment.

Sample	pH	Electrical Conductivity [mS/cm]	TOC [g/L]	TC [g/L]	IC [g/L]
Before HTC treatment					
M	6.11	0.02	0.00	0.01	0.01
MA	2.58	1.51	20.49	20.50	0.01
After HTC treatment					
M	3.82	0.51	2.65	2.67	0.02
MA	2.70	2.57	26.58	26.75	0.17

Based on our data and the literature, there are promising prospects for the valorization of process water [38], including the recovery of valuable chemicals and nutrients [39,40], the production of biogas through anaerobic digestion [41,42], or its recirculation into the process [43,44], enabling closed-loop recycling. However, further extensive and rigorous characterizations are necessary to determine the optimal valorization pathway and maximize its potential benefits.

4. Conclusions

Hydrothermal carbonization has great potential as a process suitable for the environmentally sound management of waste characterized by the dual challenge of being an infectious risk and made of various polymers. Indeed, HTC makes it possible to destroy the pathogens present in the masks and simultaneously recycle the different polymers present without the need to handle the waste to separate them. The operating conditions used in this study met the criteria found in the literature for destroying pathogens. Furthermore, the results show that the original multipolymer matrix could be converted into a material that has improved characteristics of interest in terms of reduced volume, heating value and energy density, chemical structure, and composition, especially when acetic acid is added to the liquid medium. In particular, the produced hydrochar exhibits a high calorific value while being enriched in carbon. Substitution of fossil fuels by such a secondary fuel will avoid CO₂ emissions per energy unit developed during combustion.

Moreover, when a solution of acetic acid was used as the liquid process phase, a crystal phase was produced that was identified as terephthalic acid, a value-added chemical usable in synthetic fiber production (e.g., as a precursor for the production of the same surgical mask).

It is believed that the preliminary results obtained could provide a knowledge basis for the application of HTC technology to additional types of residues similar to those studied, such as hospital waste or other categories of synthetic polymer residues that are not managed or can be managed through supply chain consortia. Applying HTC technology to these additional categories of residues would allow their valorization without the need

for complex operations of classification, separation, and cleaning that would be required in material recovery facilities. Furthermore, the environmental impact would be significantly reduced compared to currently applied management systems.

Further investigations are needed to assess the influence of operating conditions on the quality of the final products and on the potential uses of the produced hydrochar. Such studies should be accompanied by the assessment of the technical–economic feasibility of this innovative approach to the management of face masks used as personal protective equipment. In addition, the fate of process water should be deeply investigated in order to valorize it, such as through the extraction of valuable compounds that may be produced during the HTC process.

Author Contributions: Conceptualization, G.F., J.A.L., K.S.R., A.M., M.P. and G.C.; Methodology, G.F., M.P. and G.C.; Validation, G.F., J.A.L., K.S.R. and G.C.; Formal Analysis, G.F., C.C. (Carla Cannas) and C.C. (Claudio Cara); Investigation, G.F.; Resources, A.M. and G.C.; Data Curation, G.F. and G.C.; Writing—Original Draft Preparation, G.F., J.A.L., K.S.R., C.C. (Carla Cannas), C.C. (Claudio Cara), A.M. and G.C.; Visualization, G.F.; Supervision, J.A.L., K.S.R., A.M. and G.C.; Project Administration, G.C. All authors have read and agreed to the published version of the manuscript.

Funding: This research received no external funding.

Institutional Review Board Statement: Not applicable.

Informed Consent Statement: Not applicable.

Data Availability Statement: The data presented in this study are available on request from the corresponding authors.

Acknowledgments: We acknowledge CESA Project—Piano Sulcis for supporting the research activity. Thanks are due to Elodia Musu and CeSAR (Centro Servizi d’Ateneo per la Ricerca) of the University of Cagliari, Italy, for ESEM-EDX measurements performed with FEI Company Quanta 200 ESEM equipped with a Thermo Scientific EDX probe.

Conflicts of Interest: The authors declare no conflict of interest.

Abbreviations

ANOVA	Analysis of Variance
ARG	Antibiotic Resistance Gene
BET	Brunauer–Emmett–Teller
EC	Electrical Conductivity
FTIR	Fourier Transform Infrared Spectroscopy
HC	Hydrochar
HHV	Higher Heating Value
HTC	Hydrothermal Carbonization
IC	Inorganic Carbon
M	Hydrochar from surgical masks
MA	Hydrochar from surgical masks in presence of acetic acid
PC	Polycarbonate
PE	Polyethylene
PET	Polyethylene Terephthalate
PP	Polypropylene
PPE	Personal Protective Equipment
PS	Polystyrene
PTFE	Polytetrafluoroethylene
PVC	Polyvinyl Chloride
PW	Process Water

PXRD	Powder X-ray Diffraction
SEM	Scanning Electron Microscopy
TC	Total Carbon
TGA	Thermogravimetric Analysis
TOC	Total Organic Carbon
TPA	Terephthalic Acid
XRD	X-ray Diffraction

References

- World Health Organization; The United Nations Children’s Fund (UNICEF). *Water, Sanitation, Hygiene, and Waste Management for the COVID-19 Virus: Interim Guidance*; World Health Organization: Geneva, Switzerland, 2020.
- Dharmaraj, S.; Ashokkumar, V.; Pandiyan, R.; Halimatul Munawaroh, H.S.; Chew, K.W.; Chen, W.-H.; Ngamcharussrivichai, C. Pyrolysis: An Effective Technique for Degradation of COVID-19 Medical Wastes. *Chemosphere* **2021**, *275*, 130092. [[CrossRef](#)]
- Liang, Y.; Song, Q.; Wu, N.; Li, J.; Zhong, Y.; Zeng, W. Repercussions of COVID-19 Pandemic on Solid Waste Generation and Management Strategies. *Front. Environ. Sci. Eng.* **2021**, *15*, 115. [[CrossRef](#)]
- Yousef, S.; Eimontas, J.; Striūgas, N.; Abdelnaby, M.A. Pyrolysis Kinetic Behaviour and TG-FTIR-GC-MS Analysis of Coronavirus Face Masks. *J. Anal. Appl. Pyrolysis* **2021**, *156*, 105118. [[CrossRef](#)]
- Crespo, C.; Ibarz, G.; Sáenz, C.; Gonzalez, P.; Roche, S. Study of Recycling Potential of FFP2 Face Masks and Characterization of the Plastic Mix-Material Obtained. A Way of Reducing Waste in Times of COVID-19. *Waste Biomass Valor.* **2021**, *12*, 6423–6432. [[CrossRef](#)]
- Prata, J.C.; Silva, A.L.P.; Walker, T.R.; Duarte, A.C.; Rocha-Santos, T. COVID-19 Pandemic Repercussions on the Use and Management of Plastics. *Environ. Sci. Technol.* **2020**, *54*, 7760–7765. [[CrossRef](#)]
- Patrício Silva, A.L.; Prata, J.C.; Duarte, A.C.; Barcelò, D.; Rocha-Santos, T. An Urgent Call to Think Globally and Act Locally on Landfill Disposable Plastics under and after COVID-19 Pandemic: Pollution Prevention and Technological (Bio) Remediation Solutions. *Chem. Eng. J.* **2021**, *426*, 131201. [[CrossRef](#)] [[PubMed](#)]
- Fang, J.; Zhan, L.; Ok, Y.S.; Gao, B. Minireview of Potential Applications of Hydrochar Derived from Hydrothermal Carbonization of Biomass. *J. Ind. Eng. Chem.* **2018**, *57*, 15–21. [[CrossRef](#)]
- Brillard, A.; Kehrl, D.; Douguet, O.; Gautier, K.; Tschamber, V.; Bueno, M.-A.; Brillhac, J.-F. Pyrolysis and Combustion of Community Masks: Thermogravimetric Analyses, Characterizations, Gaseous Emissions, and Kinetic Modeling. *Fuel* **2021**, *306*, 121644. [[CrossRef](#)]
- Duangchan, A.; Samart, C. Tertiary Recycling of PVC-Containing Plastic Waste by Copyrolysis with Cattle Manure. *Waste Manag.* **2008**, *28*, 2415–2421. [[CrossRef](#)] [[PubMed](#)]
- Lee, G.; Eui Lee, M.; Kim, S.-S.; Joh, H.-I.; Lee, S. Efficient Upcycling of Polypropylene-Based Waste Disposable Masks into Hard Carbons for Anodes in Sodium Ion Batteries. *J. Ind. Eng. Chem.* **2022**, *105*, 268–277. [[CrossRef](#)]
- Ro, K.S.; Hunt, P.G.; Jackson, M.A.; Compton, D.L.; Yates, S.R.; Cantrell, K.; Chang, S. Co-Pyrolysis of Swine Manure with Agricultural Plastic Waste: Laboratory-Scale Study. *Waste Manag.* **2014**, *34*, 1520–1528. [[CrossRef](#)]
- Adolfsson, K.H.; Lin, C.; Hakkarainen, M. Microwave Assisted Hydrothermal Carbonization and Solid State Postmodification of Carbonized Polypropylene. *ACS Sustain. Chem. Eng.* **2018**, *6*, 11105–11114. [[CrossRef](#)]
- Ducey, T.F.; Collins, J.C.; Ro, K.S.; Woodbury, B.L.; Griffin, D.D. Hydrothermal Carbonization of Livestock Mortality for the Reduction of Pathogens and Microbially-Derived DNA. *Front. Environ. Sci. Eng.* **2017**, *11*, 9. [[CrossRef](#)]
- Funke, A.; Ziegler, F. Hydrothermal Carbonization of Biomass: A Summary and Discussion of Chemical Mechanisms for Process Engineering. *Biofuels Bioprod. Bioref.* **2010**, *4*, 160–177. [[CrossRef](#)]
- Libra, J.A.; Ro, K.S.; Kammann, C.; Funke, A.; Berge, N.D.; Neubauer, Y.; Titirici, M.-M.; Fühner, C.; Bens, O.; Kern, J.; et al. Hydrothermal Carbonization of Biomass Residuals: A Comparative Review of the Chemistry, Processes and Applications of Wet and Dry Pyrolysis. *Biofuels* **2011**, *2*, 71–106. [[CrossRef](#)]
- Shen, Y. A Review on Hydrothermal Carbonization of Biomass and Plastic Wastes to Energy Products. *Biomass Bioenergy* **2020**, *134*, 105479. [[CrossRef](#)]
- Poerschmann, J.; Weiner, B.; Wosizdlo, S.; Koehler, R.; Kopinke, F.-D. Hydrothermal Carbonization of Poly(Vinyl Chloride). *Chemosphere* **2015**, *119*, 682–689. [[CrossRef](#)]
- Shen, Y.; Yu, S.; Ge, S.; Chen, X.; Ge, X.; Chen, M. Hydrothermal Carbonization of Medical Wastes and Lignocellulosic Biomass for Solid Fuel Production from Lab-Scale to Pilot-Scale. *Energy* **2017**, *118*, 312–323. [[CrossRef](#)]
- Yao, Z.; Ma, X. Characteristics of Co-Hydrothermal Carbonization on Polyvinyl Chloride Wastes with Bamboo. *Bioresour. Technol.* **2018**, *247*, 302–309. [[CrossRef](#)]
- Xu, Z.; Bai, X. Microplastic Degradation in Sewage Sludge by Hydrothermal Carbonization: Efficiency and Mechanisms. *Chemosphere* **2022**, *297*, 134203. [[CrossRef](#)]
- Wei, Y.; Fakudze, S.; Zhang, Y.; Ma, R.; Shang, Q.; Chen, J.; Liu, C.; Chu, Q. Co-Hydrothermal Carbonization of Pomelo Peel and PVC for Production of Hydrochar Pellets with Enhanced Fuel Properties and Dechlorination. *Energy* **2022**, *239*, 122350. [[CrossRef](#)]

23. Poerschmann, J.; Weiner, B.; Wedwitschka, H.; Baskyr, I.; Koehler, R.; Kopinke, F.-D. Characterization of Biocoals and Dissolved Organic Matter Phases Obtained upon Hydrothermal Carbonization of Brewer's Spent Grain. *Bioresour. Technol.* **2014**, *164*, 162–169. [[CrossRef](#)]
24. Zhao, X.; Zhou, H.; Sikarwar, V.S.; Zhao, M.; Park, A.-H.A.; Fennell, P.S.; Shen, L.; Fan, L.-S. Biomass-Based Chemical Looping Technologies: The Good, the Bad and the Future. *Energy Environ. Sci.* **2017**, *10*, 1885–1910. [[CrossRef](#)]
25. Cywar, R.M.; Rorrer, N.A.; Hoyt, C.B.; Beckham, G.T.; Chen, E.Y.-X. Bio-Based Polymers with Performance-Advantaged Properties. *Nat. Rev. Mater.* **2021**, *7*, 83–103. [[CrossRef](#)]
26. Huang, Y.W.; Chen, M.Q.; Li, Q.H.; Xing, W. A Critical Evaluation on Chemical Exergy and Its Correlation with High Heating Value for Single and Multi-Component Typical Plastic Wastes. *Energy* **2018**, *156*, 548–554. [[CrossRef](#)]
27. Linstrom, P. NIST Chemistry WebBook, NIST Standard Reference Database 69. *J. Phys. Chem. Ref. Data Monogr.* **1998**, *9*, 1–1951.
28. Ali, L.; Kuttiyathil, M.S.; Altarawneh, M. Catalytic Upgrading of the Polymeric Constituents in COVID-19 Masks. *J. Environ. Chem. Eng.* **2022**, *10*, 106978. [[CrossRef](#)]
29. Krylova, V.; Dukštienė, N. Synthesis and Characterization of Ag₂S Layers Formed on Polypropylene. *J. Chem.* **2013**, *2013*, 987879. [[CrossRef](#)]
30. Stuart, B. *Infrared Spectroscopy: Fundamentals and Applications*; Analytical techniques in the sciences; J. Wiley: Chichester, UK; Hoboken, NJ, USA, 2004; ISBN 978-0-470-85427-3.
31. Chiu, F.-C.; Chu, P.-H. Characterization of Solution-Mixed Polypropylene/Clay Nanocomposites without Compatibilizers. *J Polym Res* **2006**, *13*, 73–78. [[CrossRef](#)]
32. Ravichandran, S.A.; Rajan, V.P.; Aravind, P.V.; Seenivasan, A.; Prakash, D.G.; Ramakrishnan, K. Characterization of Terephthalic Acid Monomer Recycled from Post-Consumer PET Polymer Bottles. *Macromol. Symp.* **2016**, *361*, 30–33. [[CrossRef](#)]
33. van Leeuwen, P.W.N.M. Catalysis, Homogeneous. In *Encyclopedia of Physical Science and Technology*; Elsevier: Amsterdam, The Netherlands, 2003; pp. 457–490. ISBN 978-0-12-227410-7.
34. Zhou, J.-H.; Shen, G.-Z.; Zhu, J.; Yuan, W.-K. Terephthalic Acid Hydropurification over Pd/C Catalyst. In *Studies in Surface Science and Catalysis*; Elsevier: Amsterdam, The Netherlands, 2006; Volume 159, pp. 293–296. ISBN 978-0-444-51733-3.
35. Cosimbescu, L.; Merkel, D.R.; Darsell, J.; Petrossian, G. Simple But Tricky: Investigations of Terephthalic Acid Purity Obtained from Mixed PET Waste. *Ind. Eng. Chem. Res.* **2021**, *60*, 12792–12797. [[CrossRef](#)]
36. Kang, M.J.; Yu, H.J.; Jegal, J.; Kim, H.S.; Cha, H.G. Depolymerization of PET into Terephthalic Acid in Neutral Media Catalyzed by the ZSM-5 Acidic Catalyst. *Chem. Eng. J.* **2020**, *398*, 125655. [[CrossRef](#)]
37. Lee, H.L.; Chiu, C.W.; Lee, T. Engineering Terephthalic Acid Product from Recycling of PET Bottles Waste for Downstream Operations. *Chem. Eng. J. Adv.* **2021**, *5*, 100079. [[CrossRef](#)]
38. Kambo, H.S.; Minaret, J.; Dutta, A. Process Water from the Hydrothermal Carbonization of Biomass: A Waste or a Valuable Product? *Biomass Valor.* **2018**, *9*, 1181–1189. [[CrossRef](#)]
39. Alhndi, M.-J.; Wüst, D.; Funke, A.; Hang, L.; Kruse, A. Fate of Nitrogen, Phosphate, and Potassium during Hydrothermal Carbonization and the Potential for Nutrient Recovery. *ACS Sustain. Chem. Eng.* **2020**, *8*, 15507–15516. [[CrossRef](#)]
40. Crossley, O.P.; Thorpe, R.B.; Peus, D.; Lee, J. Phosphorus Recovery from Process Waste Water Made by the Hydrothermal Carbonisation of Spent Coffee Grounds. *Bioresour. Technol.* **2020**, *301*, 122664. [[CrossRef](#)] [[PubMed](#)]
41. Farru, G.; Cappai, G.; Carucci, A.; De Gioannis, G.; Asunis, F.; Milia, S.; Muntoni, A.; Perra, M.; Serpe, A. A Cascade Biorefinery for Grape Marc: Recovery of Materials and Energy through Thermochemical and Biochemical Processes. *Sci. Total Environ.* **2022**, *846*, 157464. [[CrossRef](#)] [[PubMed](#)]
42. Farru, G.; Asquer, C.; Cappai, G.; De Gioannis, G.; Melis, E.; Milia, S.; Muntoni, A.; Piredda, M.; Scano, E.A. Hydrothermal Carbonization of Hemp Digestate: Influence of Operating Parameters. *Biomass Conv. Bioref.* **2022**, 1–12. [[CrossRef](#)]
43. Chen, X.; Ma, X.; Peng, X.; Lin, Y.; Wang, J.; Zheng, C. Effects of Aqueous Phase Recirculation in Hydrothermal Carbonization of Sweet Potato Waste. *Bioresour. Technol.* **2018**, *267*, 167–174. [[CrossRef](#)]
44. Arauzo, P.J.; Olszewski, M.P.; Wang, X.; Pfersich, J.; Sebastian, V.; Manyà, J.; Hedin, N.; Kruse, A. Assessment of the Effects of Process Water Recirculation on the Surface Chemistry and Morphology of Hydrochar. *Renew. Energy* **2020**, *155*, 1173–1180. [[CrossRef](#)]

Disclaimer/Publisher's Note: The statements, opinions and data contained in all publications are solely those of the individual author(s) and contributor(s) and not of MDPI and/or the editor(s). MDPI and/or the editor(s) disclaim responsibility for any injury to people or property resulting from any ideas, methods, instructions or products referred to in the content.